Chinese Chemical Letters 31 (2020) 2980–2984

Contents lists available at ScienceDirect

Chinese Chemical Letters

journal homepage: www.elsevier.com/locate/cclet

Communication

# Molecular engineering of ultra-sensitive fluorescent probe with large Stokes shift for imaging of basal HOCl in tumor cells and tissues

Peng Lu[1], Xingxing Zhang[1], Tianbing Ren, Lin Yuan*

*State Key Laboratory of Chemo/Biosensing and Chemometrics, College of Chemistry and Chemical Engineering, Hunan University, Changsha 410082, China*

ARTICLE INFO

*Article history:*
Received 16 June 2020
Received in revised form 8 August 2020
Accepted 12 August 2020
Available online 13 August 2020

*Keywords:*
Fluorescent probes
High sensitivity
Hypochlorous acid (HOCl)
Large Stokes shift
Fluorescence imaging

ABSTRACT

Fluorescent probes have been widely employed in biological imaging and sensing. However, it is always a challenge to design probes with high sensitivity. In this work, based on rhodamine skeleton, we developed a general strategy to construct sensitivity-enhanced fluorescent probe with the help of theoretical calculation for the first time. As a proof of concept, we synthesized a series of HOCl probes. Experiment results showed that with the C-9 of pyronin moiety of rhodamine stabilized by an electron donor group, probe DQF-S exhibited an importantly enhanced sensitivity (LOD: 0.2 nmol/L) towards HOCl together with fast response time (<10 s). Moreover, due to the breaking symmetrical electron distribution by another electron donor group, the novel rhodamine probe DQF-S displayed a far red to near-infrared emission (>650 nm) and large Stokes shift. Bioimaging studies indicated that DQF-S can not only effectively detect basal HOCl in various types of cells, but also be successfully applied to image tumor tissue *in vivo*. These results demonstrate the potential of our design as a useful strategy to develop excellent fluorescent probes for bioimaging.



Fluorescent probes, owing to their simple operation, non-invasive nature, high sensitivity, and fine spatiotemporal resolution, *etc*., have been one of the most important tools for bioimaging [1–6]. So far, various fluorophores have been used as signaling units to construct fluorescent probes [7–11]. Among them, rhodamine and its derivatives are particularly popular scaffolds for developing high contrast probes due to an equilibrium between an open, highly fluorescent quinoid form and a closed, nonfluorescent lactone (Fig. 1a) [8,12]. Moreover, owing to their cationic character, these dyes generally have good water solubility and cell membrane permeability, which is very beneficial for rapid cellular uptake and imaging [13]. However, due to the short emission wavelength (usually between 500 nm and 600 nm) and small Stokes shifts, most of the traditional rhodamine probes suffer from serious auto-fluorescence and self-quenching, resulting in significantly compromised signal-to-noise ratio [14,15]. Importantly, the fluorescent probes based on the spirocyclization of traditional rhodamines usually display a delayed response time [16–23], and the relationship between their structure and probe's sensitivity is still unknown, which severely hinders their further application in biological imaging. Therefore, it is significant and necessary to develop a general strategy that could solve these problems.

Hypochlorous acid (HOCl) is an important reactive oxygen species (ROS), which is formed by per-oxidation of chloride ions with the catalysis of myeloperoxidase (MPO) and can serve as a "killer" for pathogens in the innate immune system [24–26]. In physiological condition, the average produced level of HOCl is about 0.47 nmol/min per $10^6$ cells [27,28]. However, aberrant generation of HOCl would lead to various clinical diseases, such as Parkinson's disease [29], cerebral ischemia [30] and cancers [26,31]. Thus, it is imperative to develop effective fluorescent probes to track HOCl and investigate its role in related diseases in living systems.

In this work, by introducing electron donor onto the conjugated structure with the help of theoretical calculation, we describe a general strategy to develop highly sensitive rhodamine probe (Fig. 1b). Moreover, due to the break of symmetrical electron distribution, the novel rhodamine probe exhibits large Stokes shift accompanied with far red to near-infrared emission (> 650 nm). To verify the advantages of the novel rhodamine probe in living system, we then constructed a HOCl fluorescent probe DQF-S. Bioimaging studies indicated that probe DQF-S could quickly enter the cells (within 3 min) and effectively react with the basal HOCl in cancer cells. Furthermore, benefiting from its far red to NIR emission, DQF-S was also successfully applied to image HOCl in tumor tissue and live mice.

* Corresponding author.
*E-mail address:* lyuan@hnu.edu.cn (L. Yuan).
[1] These authors contributed equally to this work.

https://doi.org/10.1016/j.cclet.2020.08.016
1001-8417/

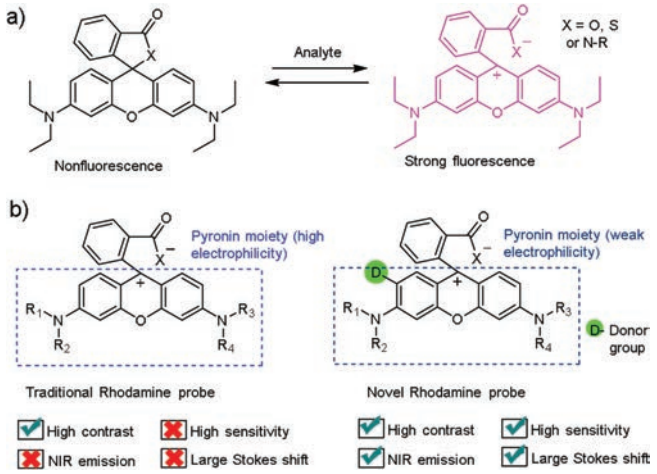


**Fig. 1.** (a) Structures of traditional rhodamine and the equilibrium between its spirolactone and ring-opening form. (b) Chemical structures of traditional and novel rhodamine probes.

Rhodamines, owing to their outstanding photophysical properties such as high extinction coefficients and quantum yields, and excellent photostability, have been widely used for fluorescent probe design [8]. Although as popular as they are, most of those probes suffer from poor sensitivity and delayed response to the signalling elements. We reason that the electronics deficiency of the pyronin moiety, especially the lack of electrons on C-9, hindered the open loop of the traditional rhodamine probes. Thus, we conjecture that if we can stabilize C-9, the response performance of the rhodamine probes (including sensitivity and response time) could be effectively enhanced. Conversely, enhancing the C-9's positive charge will reduce their response performance. To prove our conjecture, we choose and design three kinds of rhodamine dyes (Fig. 2a). Density functional theory (DFT) calculations indicate that the charge on C-9 of traditional rhodamine B is 0.128 (NBO charge). However, with the strong electron donor group amine modified at C-7 position, the novel rhodamine DQF-RB exhibits an obvious charge reduction at C-9 (0.107). In contrast, if we reduce the electron donating ability of the amine group at the C-3 position and introduce a phenothiazine unit at the C-7 and C-6 position, the charge on C-9 of the novel rhodamine PZQ-R6G would increase up to 0.132. As proof of concept, we designed and synthesized three probes for detecting HOCl based on above rhodamine derivatives (Fig. 2b). The synthetic route was as described in Scheme S1 (Supporting information). The probes were synthesized by the reaction of rhodamine dyes with Lawesson's reagent and then confirmed by ESI and NMR analyses (Supporting information).

To compare the responsiveness of the three probes, we firstly titrated HOCl to the PBS solution (containing 50% EtOH, pH 7.4) of the probes from 0 μmol/L to 20 μmol/L. As shown in Fig. 3a and Figs. S1–S3 (Supporting information), based on the traditional rhodamine B scaffold, probe RB-S showed 15-fold enhancement of the fluorescence signal ($F/F_0$) at 585 nm when 20 μmol/L HOCl was added. However, as we expected, with an electron donor group decorated, probe DQF-S has a significant signal enhancement, about 500-fold enhancement with 20 μmol/L HOCl treated. Importantly, even with only 1 μmol/L HOCl added, the fluorescence enhancement of DQF-S can also be reached up to 78-fold, which is about 5 times than that of probe RB-S with 20 μmol/L HOCl added (Fig. 3a and Figs. S1–S3). These results demonstrated that stabilizing C-9 of the pyronin part of rhodamine with an electron donor group can indeed enhance the sensitivity of the rhodamine probe. On the other hand, compared to traditional probe RB-S, DQF-S exhibited a large Stokes shift (81 nm) and NIR emission (677 nm), which can effectively enhance tissue penetration depth, minimize autofluorescence and self-quenching [14,32]. In addition, it can be clearly seen that when the charge on C-9 of the pyronin moiety of rhodamine was increased in PZQ-R6G, probe PZQ-S displayed no response in the presence of 20 μmol/L HOCl (Fig. 3a and Figs. S1–S3). This further illustrated that stabilized C-9 of the pyronin part is very important and can effectively increase the sensitivity of rhodamine probe.

Based on above results, we further explored the detection limit, selectivity, and response time of DQF-S to HOCl. As shown in Fig. 3b, DQF-S (5 μmol/L) is essentially non-fluorescence. When a low concentration of HOCl from 0 μmol/L to 1 μmol/L was added, the fluorescence signal ($F/F_0$) of DQF-S at 677 nm was gradually enhanced and showed a linear response (Fig. 3b and Fig. S4 in Supporting information). According to the formula (3 × standard deviation/slope), the detection limit of probe DQF-S was calculated to be 0.2 nmol/L, which is much lower than RB-S (80 nmol/L) and

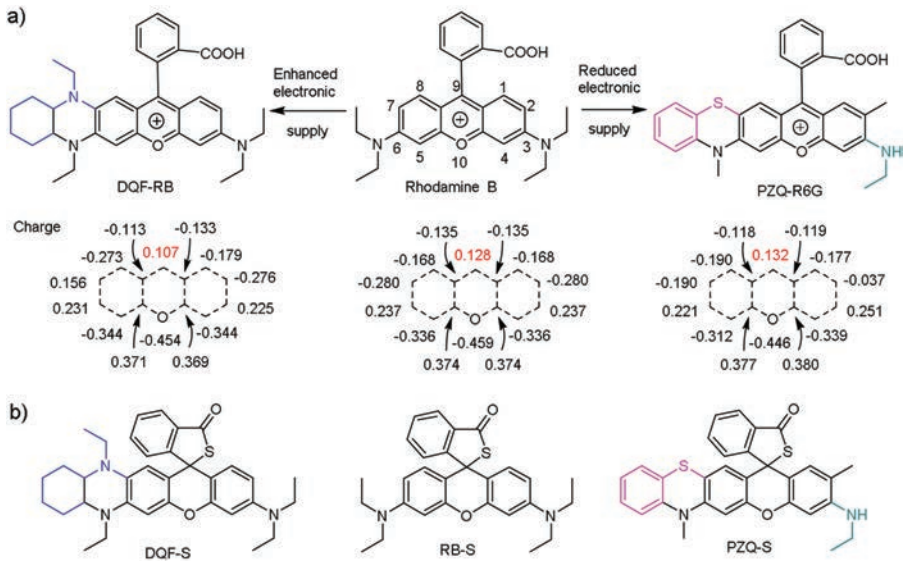


**Fig. 2.** (a) Rational engineering principle of novel rhodamine probes and the charge (NBO charge) distribution on their pyronin rings. (b) Chemical structures of the three HOCl probes.

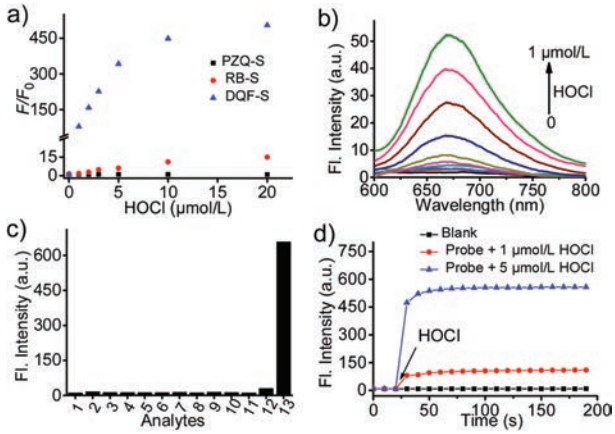


**Fig. 3.** Fluorescence spectra of DQF-S (5 μmol/L) responding towards HOCl in ethanol/PBS (1:1, pH 7.4) solution. (a) Fluorescence intensity ratio ($F/F_0$) of DQF-S, RB-S and PZQ-S to the concentration of HOCl, data was acquired immediately after HOCl addition. The excitation wavelength of these probes was at their optimal excitation wavelength. (b) Fluorescence enhancement of DQF-S upon addtion of low concentrations of HOCl (0-1 μmol/L). (c) Fluorescence intensity of DQF-S to HOCl (5 μmol/L) and other analytes: 1-13: blank, GSH (1 mmol/L), Cys (50 μmol/L), $Fe^{3+}$ (50 μmol/L), $H_2O_2$ (100 μmol/L), *t*-BuOO$^{\bullet}$ (100 μmol/L), NO$^{\bullet}$ (100 μmol/L), $O_2^{\bullet-}$ (100 μmol/L), $H_2S$ (100 μmol/L), $Na_2SO_3$ (100 μmol/L), OH$^{\bullet}$ (100 μmol/L), $ONOO^-$ (5 μmol/L), HOCl (5 μmol/L). (d) Time course of fluorescence intensity of DQF-S after adding 1 μmol/L and 5 μmol/L HOCl. $\lambda_{ex}$ = 580 nm.

PZQ-S (> 20 μmol/L) as well as those of the known HOCl probes (Tables S1 and S2 in Supporting information), indicating that DQF-S has a great potential to detect trace amounts of HOCl in living cells.

To investigate the selectivity, various interfering reactive species ($H_2O_2$,*t*-BuOO$^{\bullet}$, NO$^{\bullet}$, $O_2^{\bullet-}$, $H_2S$ $Na_2SO_3$, $^{\bullet}$OH, ONOO) and biomolecules (GSH, Cys, $Fe^{3+}$) were added to the PBS solution (containing 50% EtOH, pH 7.4) of probe DQF-S (5 μmol/L). As shown in Fig. 3c, even with excess concentrations than that of living cells, the fluorescence intensity of DQF-S at 677 nm had hardly changes towards the other active molecules, compared with 5 μmol/L HOCl. Time-course studies revealed that DQF-S has a very rapid response to HOCl, the reaction can be completed within seconds (Fig. 3d), which is much faster than those of the known HOCl probes (Table S2 in Supporting information). In addition, DQF-S exhibited good stability in the range of pH 4–9, which proved that the response was indeed caused by HOCl (Fig. S5 in Supporting information). All these results indicated that probe DQF-S is an excellent HOCl probe with high sensitivity, superior selectivity, and fast response, and is very feasible for the real-time detection of HOCl in living system.

Encouraged by the promising experimental results *in vitro*, we further studied the performance of DQF-S in biological system. Before the cell experiments, we first studied the biocompatibility of DQF-S, the MTT assay showed that DQF-S has negligible effect on cell viability at the concentration range of 1–10 μmol/L after 24 h of incubation (Fig. S6 in Supporting information). Then exogenous experiments were conducted, as shown in Fig. S7 (Supporting information), live L02 cells incubated with 5 μmol/L DQF-S showed almost no fluorescence. While a significant fluorescence was observed after the cells were treated with 20 μmol/L HOCl. The exogenous cell experiment results demonstrated the efficacy of DQF-S to detect intracellular HOCl. Therefore, we next examined the applicability of DQF-S to monitor endogenous HOCl level in living cells. Fig. S8 (Supporting information) showed that DQF-S presented no fluorescence in living L02 cells regardless of the presence or absence of LPS stimulation. However, by contrasting, HeLa cells incubated with 5 μmol/L DQF-S emitted strong fluorescence signals without stimulation and showed an obvious

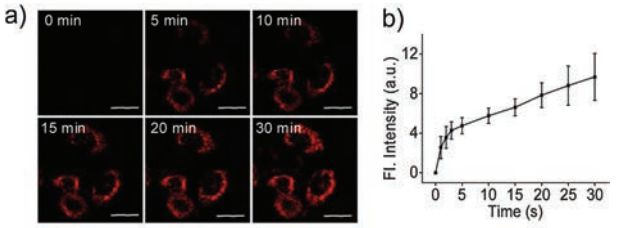


**Fig. 4.** (a) Time course of fluorescence intensity of MCF-7 cells after addtion of 5 μmol/L DQF-S. (b) Average intensity in image a, respectively. Error bars are standard deviation (SD). The excitation wavelength was 561 nm. The emission band was at 600-700 nm. Scale bar: 20 μm.

increase in fluorescence intensity after treated with LPS (Fig. S8). This may be reasoned for that L02 cells (hepatocyte cells) lack of MPO enzymes and therefore cannot synthesize HOCl [33]. For HeLa cells, we assumed that it is not only because of the presence of MPO enzymes, but also due to the higher levels of HOCl in HeLa cells [27]. After stimulation, the increased levels of HOCl once again proved the existence of MPO enzyme in HeLa cells, and also confirmed the availability of DQF-S in monitoring endogenous HOCl level in living cells. In addition, colocalization experiments showed that probe DQF-S mainly concentrated in mitochondria (Fig. S9 in Supporting information), indicating that DQF-S has potential to mitochondrial HOCl detecting.

Based on the above results, we next investigated the ability of probe DQF-S to be taken up by living cells and real-time image endogenous HOCl. As shown in Fig. 4a and Fig. S10 (Supporting information), MCF-7 cells showed almost no fluorescent signal after the addition of 5 μmol/L DQF-S. However, a significant fluorescence signal was observed after a few minutes. Moreover, the fluorescence intensity increased over time. The large slope of the fluorescence intensity curve in the first few minutes (only about 3 min) indicated that probe DQF-S can quickly enter cells and sensitively respond with intracellular HOCl. However, due to the continuous production of HOCl in living cells, the fluorescence intensity of DQF-S would also gradually increase after the probe entered the cells (3–30 min) (Fig. 4b and Fig. S10 in Supporting information). The linear response between emission intensity and HOCl indicated that DQF-S possesses great potential to quantify the concentration of HOCl in living cells.

Usually, the concentration of basal HOCl for each cell line is unequal. Encouraged by the above results, we further verified whether probe DQF-S is enough sensitive to distinguish the difference of the basal HOCl in various cells. We selected three types of cancer cells (HeLa, MCF-7 and MDA231), two kinds of normal cells (L02 and HEK293) and one kind of immune cells (RAW264.7) as research models. As shown in Fig. 5a, after incubation of the cells with 5 μmol/L DQF-S for 20 min, cancer cells exhibited strong fluorescence. In contrast, almost no fluorescence was observed in the normal cells, and RAW264.7 cells showed weak fluorescence. Theses results indicated that the basal HOCl levels in cancer cells (HeLa, MCF-7, and MDA-MB-231) are much higher than that of non-cancer cells (L02, HEK293, and RAW264.7), especially for normal cells (HEK293). This may be due to the fact that cancer cells are under higher levels of oxidative stress than normal cells, which leads to increased ROS (such as HOCl, $ONOO^-$, $H_2O_2$) in cancer cells and in turn triggered alterations in metabolism and oncogenic transformation [34,35]. In addition, it should also be noted that there is obvious differences in fluorescence intensity for different types of cancer cells. As shown in Fig. 5b, the MCF-7 cells showed the strongest fluorescence, followed by MDA-MB-231 cells, and HeLa cells showed relatively low fluorescence. To confirm that the increase in fluorescence intensity was indeed caused by HOCl, we precultured MCF-7 cells with 4-aminobenoic acid hydrazide (ABAH, a myeloperoxidase inhibitor)

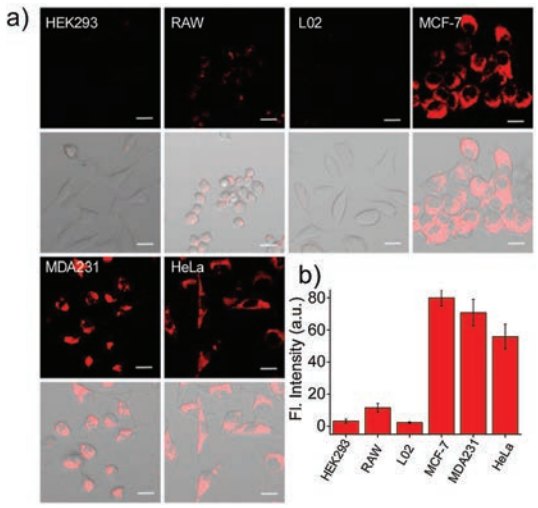


**Fig. 5.** (a) Fluorescence imaging and fluorescence-transmission overlay imaging of normal cells (HEK293, RAW, L02) and cancer cells (MCF-7, MDA231, HeLa) stained with 5 μmol/L DQF-S for 20 min. (b) Average fluorescence intensity of different cells in images of a. The emission band was collected at 600-700 nm, $\lambda_{ex}$ = 561 nm, Scale bar: 20 μm.

and a significant fluorescence reduction was observed (Fig. S11 in Supporting information). These results indicated that DQF-S was a useful tool, which can not only effectively distinguish the cancer cells from non-cancer cells, but also identified the different types of cancer cells by detecting their basal HOCl.

As an additional showcase of the application, we subsequently mixed cancer cells and normal cells to construct a simulated tumor environment. Herein, we selected MCF-7 cells and L02 cells which have obvious morphological differences. As shown in Fig. S12 (Supporting information), after incubation of DQF-S for 20 min, cells with different brightness and darkness state were observed by the confocal microscope. Compared to L02 cells exhibiting non-fluorescence, MCF-7 cells displayed significant fluorescence at the channel of 600−700 nm. This phenomenon can also be achieved by flow cytometry (Fig. S13 in Supporting information). The significant difference in fluorescence intensity reached our expectations and further demonstrated the potential of DQF-S to distinguish cancer cells from normal cells.

Considering that the NIR emission (> 650 nm) has enhanced tissue penetration and reduced tissue background fluorescence [15,36], we then validate the possibility of probe DQF-S for *in vivo* imaging. By subcutaneous injection of cancer cells MCF-7, we established a tumor model into the armpits of nude mice. As shown in Fig. S14 (Supporting information), with DQF-S injected *in situ*, the tumor in living mice exhibited a strong fluorescence, while the normal tissue remained largely negative. To confirm the tumor signal was indeed derived from the tissue within the tumor, we then dissected the tumor from the nude mice for further imaging. Living imaging system and confocal microscope displayed that tumor tissue exhibited much stronger fluorescence than normal tissue, indicating there is a much higher level of HOCl in tumor tissue than that of normal tissue. This result is in good according with our above investigation. All these biological experiments confirmed that DQF-S can be employed as an efficient NIR HOCl probe for imaging tumor tissue *in vivo*.

In summary, we report in this study a novel strategy to develop highly sensitive rhodamine probe with far red to NIR emission. With the electron donor introduced onto pyronin part, the novel rhodamine probe DQF-S not only exhibited an importantly enhanced sensitivity (LOD: 0.2 nmol/L), but also showed rapid response (< 10 s) towards HOCl in near-infrared region together with a large Stokes shift. Cells imaging indicated that DQF-S could quickly enter the cells and holds the ability to detect both exogenous and endogenous HOCl in cells. In particular, the probe is efficient to detect basal HOCl in cancer cells, and rationally be applied to distinguish cancer cells from non-cancer cells. The result was future confirmed by co-culture of MCF-7 cells and L02 cells. Moreover, NIR emission enabled probe DQF-S further applicable *in vivo* and tissue imaging. We believe that our strategy not only can be used to develop excellent HOCl fluorescent probes, but also largely contributes to future designs of other highly sensitive rhodamine probes.

## Declaration of competing interest

We declare that we have no financial and personal relationships with other people or organizations that can inappropriately influence our work, there is no professional or other personal interest of any nature or kind in any product, service and/or company that could be construed as influencing the position presented in, or the review of, the manuscript entitled.

## Acknowledgments

This work is supported by the National Natural Science Foundation of China (Nos. 21877029, 21735001), the National Key R&D Program of China (No. 2019YFA0210103), the National Postdoctoral Program for Innovative Talents (No. BX20190110) and the China Postdoctoral Science Foundation (No. 2019M662758).

## Appendix A. Supplementary data

Supplementary material related to this article can be found, in the online version, at doi:https://doi.org/10.1016/j.cclet.2020.08.016.

## References

[1] W. Xu, Z. Zeng, J.H. Jiang, Y.T. Chang, L. Yuan, Angew. Chem. Int. Ed. 55 (2016) 13658–13699.
[2] H.W. Liu, L. Chen, C. Xu, et al., Chem. Soc. Rev. 47 (2018) 7140–7180.
[3] X. Wu, W. Shi, X. Li, H. Ma, Acc. Chem. Res. 52 (2019) 1892–1904.
[4] D. Chen, W.J. Qin, H.X. Fang, et al., Chin. Chem. Lett. 30 (2019) 1738–1744.
[5] G.D. Hu, H.Y. Jia, L.N. Zhao, D.H. Cho, J.G. Fang, Chin. Chem. Lett. 30 (2019) 1704–1716.
[6] H. Zhou, S.S. Li, X.D. Zeng, et al., Chin. Chem. Lett. 31 (2020) 1382–1386.
[7] W. Li, X. Gong, X. Fan, et al., Chin. Chem. Lett. 30 (2019) 1775–1790.
[8] L. Wang, W. Du, Z. Hu, et al., Angew. Chem. Int. Ed. 58 (2019) 14026–14043.
[9] L. Wang, M.S. Frei, A. Salim, K.J. Johnsson, Am. Chem. Soc. 141 (2019) 2770–2781.
[10] B.J. Bezner, L.S. Ryan, A.R. Lippert, Anal. Chem. 92 (2020) 309–326.
[11] J. Yang, K. Li, J.T. Hou, et al., Sci. China Chem. 60 (2017) 793.
[12] M. Beija, C.A.M. Afonso, J.M.G. Martinho, Chem. Soc. Rev. 38 (2009) 2410–2433.
[13] M. Li, S. Long, Y. Kang, et al., Am. Chem. Soc. 140 (2018) 15820–15826.
[14] T.B. Ren, W. Xu, W. Zhang, et al., J. Am. Chem. Soc. 140 (2018) 7716–7722.
[15] D. Cheng, J. Peng, Y. Lv, et al., J. Am. Chem. Soc. 141 (2019) 6352–6361.
[16] L. Yuan, W. Lin, Y. Xie, B. Chen, J. Song, Chem. Eur. J. 18 (2012) 2700–2706.
[17] X. Chen, X. Wang, S. Wang, et al., Chem. Eur. J. 14 (2008) 4719–4724.
[18] S. Kenmoku, Y. Urano, H. Kojima, T.J. Nagano, Am. Chem. Soc. 129 (2007) 7313–7318.
[19] Q. Xu, K.A. Lee, S. Lee, et al., J. Am. Chem. Soc. 135 (2013) 9944–9949.
[20] X. Wu, Z. Li, L. Yang, J. Han, S. Han, Chem. Sci. 4 (2013) 460–467.
[21] Y. Tang, G.F. Jiang, Tetrahedron Lett. 58 (2017) 2846–2849.
[22] Y. Wang, H. Ding, Z. Zhu, et al., J. Photochem. Photobiol. A: Chem. 390 (2020) 112302.
[23] F. Song, X. Shao, J. Zhu, et al., Tetrahedron Lett. 60 (2019) 1363–1369.
[24] L. Yuan, L. Wang, B.K. Agrawalla, et al., J. Am. Chem. Soc. 137 (2015) 5930–5938.
[25] C. Shao, J. Yuan, Y. Liu, et al., Proc. Natl. Acad. Sci. U. S. A. 117 (2020) 10155–10164.
[26] J. Wang, D. Cheng, L. Zhu, et al., Chem. Commun. 55 (2019) 10916–10919.
[27] H. Zhu, J. Fan, J. Wang, H. Mu, X. Peng, J. Am. Chem. Soc. 136 (2014) 12820–12823.
[28] Y. Aratani, H. Koyama, S.I. Nyui, et al., Infect. Immun. 67 (1999) 1828–1836.
[29] D.K. Choi, S. Pennathur, C. Perier, et al., J. Neurosci. 25 (2005) 6594–6600.
[30] M. Miljkovic-Lolic, R. Silbergleit, G. Fiskum, R.E. Rosenthal, Brain Res. 971 (2003) 90–94.
[31] P. Wei, L. Liu, W. Yuan, et al., Sci. China Chem. 63 (2020) 1153–1158, doi:http://dx.doi.org/10.1007/s11426-020-9737-y.

[32] W. Chen, S. Xu, J.J. Day, D. Wang, M. Xian, Angew. Chem. Int. Ed. 56 (2017) 16611–16615.
[33] A.J. Shuhendler, K. Pu, L. Cui, J.P. Uetrecht, J. Rao, Nat. Biotechnol. 32 (2014) 373–380.
[34] E.O. Hileman, J. Liu, M. Albitar, M.J. Keating, P. Huang, Cancer Chemoth. Pharm. 53 (2004) 209–219.
[35] L. Behrend, G. Henderson, R.M. Zwacka, Biochem. Soc. Trans. 31 (2003) 1441–1444.
[36] L. Yuan, W. Lin, K. Zheng, L. He, W. Huang, Chem. Soc. Rev. 42 (2013) 622–661.